NASA DEVELOP National Program
Maryland – Goddard

Fall 2024

Illinois Ecological Conservation

Using Earth Observations to Identify Areas of Oak Decline in Illinois and Investigate Contributing Risk Factors

DEVELOP Technical Report
November 22nd, 2024

Flora Hamilton (Project Lead, Analytical Mechanics Associates)
Nancy Nthiga (Analytical Mechanics Associates)
Emma Rubin (Analytical Mechanics Associates)
Benjamin Shostak (Analytical Mechanics Associates)

Advisors:
Sean McCartney, Science Systems & Applications, Inc., NASA Goddard Space Flight Center (Science Advisor)
Joseph P. Spruce, Analytical Mechanics Associates, NASA Langley Research Center (Science Advisor)

Lead:
Isabel Lubitz (Maryland – Goddard)

1. Abstract

Rapid white oak mortality is an increasing concern in the Midwestern United States, including Illinois, where oak forests are a key component in ecosystem functionality. The Morton Arboretum is conducting research to determine the main drivers of white oak (*Quercus alba*) decline and in turn, create plans to conserve these woodlands across Illinois. We partnered with this organization to test the feasibility of using Earth observation data and GIS technologies in determining areas of white oak decline and its drivers. We used Harmonized Landsat and Sentinel-2 and data from Landsat 5 Thematic mapper, Landsat 7 Enhanced Thematic Mapper Plus, Landsat 8 Operational Land Imager (OLI), and Landsat 9 OLI-2 to identify changes in forest canopy greenness by calculating differences in the Normalized Difference Vegetation Index (NDVI) between 2010 – 2024 in two regions of Southern Illinois: the Shawnee National Forest and Kaskaskia River Basin. We examined relationships between NDVI differences and potential drivers, including topographic, climate, and agricultural variables to compute a present-day risk map for white oak forest decline. For each study area, we identified key years of climatic stress and detected negative NDVI change within known areas of oak decline; however, more ground truth data is needed to conduct a comprehensive and unbiased accuracy assessment. Through Principal Component Analysis of risk variables, we found that drought conditions, Topographic Wetness Index, and slope emerged as the most consequential variables in both study regions for our generated risk map. Areas exhibiting high risk in the generated risk map were clustered along the eastern, central, and northwestern regions of the Shawnee National Forest, while high risk areas in Kaskaskia were more widespread.

Key Terms

remote sensing, Landsat, Harmonized Landsat Sentinel-2, white oak decline, rapid white oak mortality, Illinois, *Quercus alba*

2. Introduction

2.1 Background Information

Oak trees (*Quercus spp.*) have been an ecologically dominant species and key component of forest ecosystem functionality across the midwestern and eastern United States for the last 10,000 years (Crocker et al., 2023; Knoot et al., 2015; Novick et al., 2022). Oak forests provide numerous ecosystem services that support rich biodiversity, crucial ecological processes (e.g., carbon sequestration, nutrient and water cycling), and socioecological benefits both materially (e.g., timber products, clean air and water) and immaterially (e.g., cultural connection, recreational opportunities; Crocker et al., 2023; Novick et al., 2022). However, mature oak forest populations (e.g., stands) are increasingly threatened by a combination of stressors, including droughts, pests, and nutrient deficiencies, which are exacerbated by human-induced changes in climate and land use/land cover (Pascual et al., 2022). This is particularly evident in the eastern United States, as well as midwestern regions, including Illinois, where white oak (*Q. alba*) and other oak species decline have been attributed to invasive pests, such as oomycete pathogens, as well as an interaction of stress factors (Kamoun et al., 2014). Oak decline is a multifaceted phenomenon resulting from a combination of predisposing factors (e.g., elevation, slope, climate regime, topography), inciting factors (e.g., droughts, heat waves, precipitation, floods, and windstorm damage), and contributing factors (e.g., insects and diseases; Macháčová et al., 2022). As a result, this complexity of damage agents poses significant challenges for predicting and managing oak forest health.

In recent years, remote sensing technologies have complemented labor-intensive field survey techniques, making forest health anomaly detection more feasible and efficient. These advanced methods enable early detection of forest stress, providing crucial information for preventive measures of further distress (Hwang et al., 2023). The Normalized Difference Vegetation Index (NDVI) has been employed as a reliable indicator for monitoring the health of various oak species, as demonstrated through studies of the cork oak (*Q. suber*; El Ahmadi et al., 2023) and holm oak (*Q. ilex*; Aubard et al., 2019). This vegetative index facilitates the identification of oak mortality (as a function of forest greenness decline) through time series analysis of data from Earth-observing satellites such as Landsat and Sentinel-2 (Catalão et al., 2022). Vegetation indices from

multispectral satellite data have been used to enhance the detection of oak-dominant diseases with increased flexibility, as they utilize a reduced number of wavelengths (i.e., spectral bands) and can be calculated with multiple data collection platforms (Sapes et al., 2022). These advancements have significantly improved the ability to monitor and manage forest health on a large scale, providing valuable tools for forest managers and researchers.

2.2 Project Partners & Objectives

The Morton Arboretum, a tree-focused botanic garden and research center in Lisle, Illinois addresses the growing concern of rapid white oak mortality by conducting oak mortality research and collaborating with the Illinois Department of Natural Resources, foresters, and green industry professionals to provide pest and disease information for management of the state's forests. In 2022, the Bipartisan Infrastructure Law (Infrastructure Investment and Jobs Act, 2021) enabled further research efforts to investigate the spatial distribution and key drivers of oak decline in Illinois. Since 2023, the Morton Arboretum has been conducting surveys of vulnerable white oak stands and oomycete pathogen assessments from root tissue samples across southern Illinois, where rapid white oak mortality was recently observed. Despite these efforts, the arboretum still faces challenges in its field sampling approach. The current method of collecting mortality and root sample surveys is labor-intensive, time-consuming, costly, and only covers a limited number of sites. Additionally, accessing remote forest stands, particularly in rough terrain across southern Illinois, poses logistical difficulties for regular monitoring. These constraints make it challenging to establish a comprehensive understanding of rapid white oak mortality and implement timely management responses. Modern remote sensing techniques could complement their ground-based sampling efforts by providing broader spatial coverage and helping to locate and prioritize areas for field sampling.

To support the Morton Arboretum's sampling efforts, we assessed the feasibility of using satellite data to identify stressed oak stands requiring field inspection. Using forest NDVI change maps from two satellite sensors, combined with environmental data, our study addressed three objectives: detect changes in oak tree health through Earth observations, assess potential risk variables and their relationships to the decline in white oak health, and create a present-day oak decline risk map to help the partner prioritize areas for field investigation.

2.3 Study Area & Study Period

This project examined environmental drivers of white oak decline across two regions in Illinois with documented cases of rapid white oak mortality: the Kaskaskia River Basin and the Shawnee National Forest (Figure 1). Based on stakeholder interest, the analysis examined environmental conditions from 2010 through the summer of 2024, providing a 14-year window to investigate potential stressors contributing to current decline patterns in these areas. The Kaskaskia River Basin covers approximately 3.7 million acres across 22 counties in Illinois, representing about 10% of the state's total area (Illinois Department of Natural Resources, 2017). Agricultural land dominates the basin, accounting for 82% of the total area. Forest cover comprises about 13% of the basin, primarily concentrated along streams, hillsides, and in the southern two-thirds of the watershed (Krohe, 2001). The basin contains Illinois' largest block of contiguous forest, a 7,000-acre tract of floodplain forest and oak-dominated flatwoods, and a bottomland hardwood forest (Krohe, 2001). We also investigated the Shawnee National Forest, a mixed-use forest that spans approximately 289,000 acres between the Ohio and Mississippi Rivers in southern Illinois (United States Forest Service, n.d.-a). The region's topography is largely characterized by rugged hills and steep-sided ravines, broad bottomlands along creeks, and razorback ridges. Ecologically, oak-hickory forests largely dominate the Shawnee National Forest, with moist upland forests featuring a mix of American beech, sugar maple, and tulip poplars (United States Forest Service, n.d. -b). The two regions differ in land use and composition, providing unique perspectives for understanding regional oak mortality.

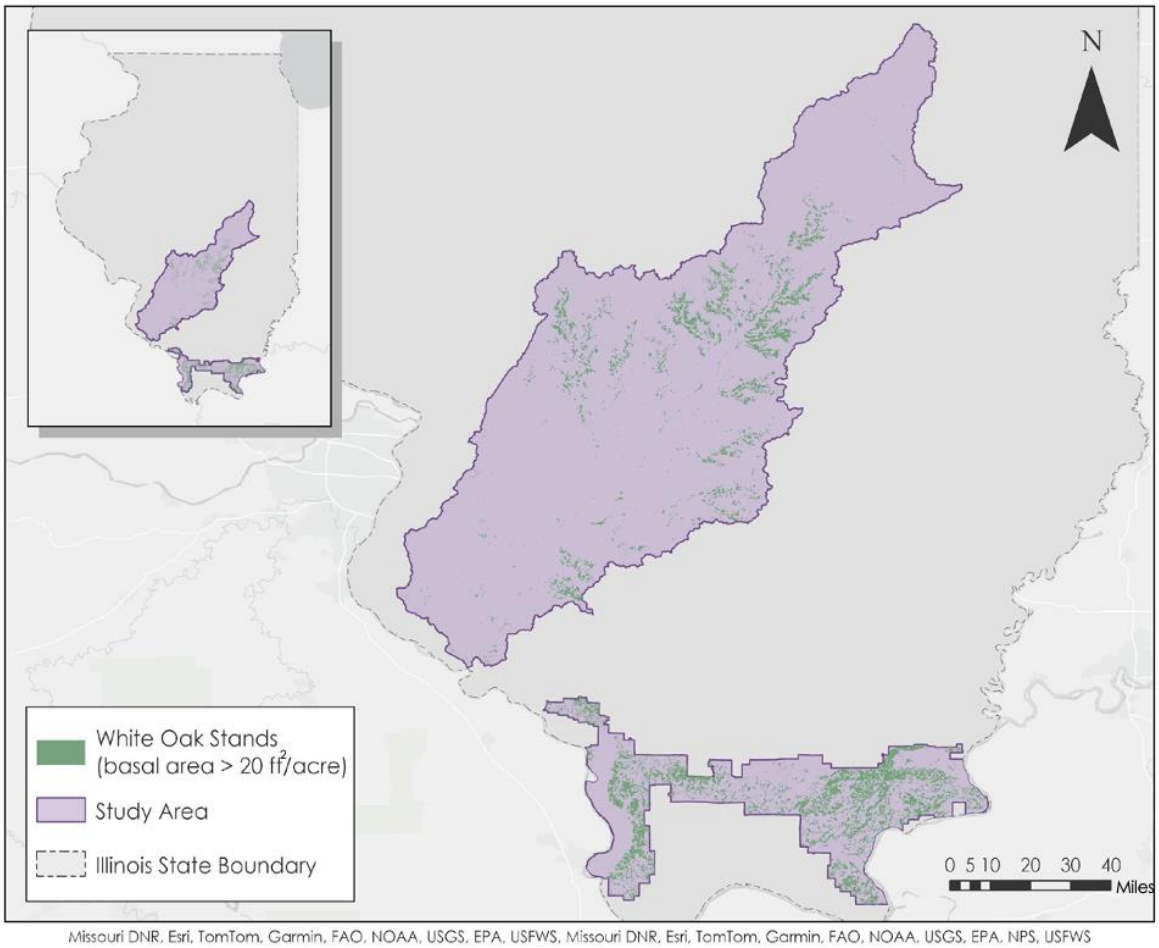

Figure 1. Map of study areas in Illinois showing the Kaskaskia River Basin (upper left, purple) and the Shawnee National Forest (lower right, purple), with modeled white oak stands (basal area >20 ft²/acre) from the United States Forest Service Individual Tree Species Parameter Map.

3. Methodology

Our approach, leveraging four key datasets, resulted in a risk assessment model for potential white oak mortality by integrating multiple environmental and climatic factors across the Kaskaskia River Basin and Shawnee National Forest regions. To achieve this, we analyzed Earth observations from multiple satellite platforms (2010 – 2024) to track vegetation health change in white oak stands through an NDVI time series analysis. Additionally, we used topographic data to understand landscape influences on water movement and aspect, as well as to capture patterns of water-borne pathogen (oomycete) buildup. Finally, we used climate data to identify drought and temperature stress patterns and cropland data to assess possible herbicide pollution impacts on oak forest health.

We analyzed NDVI change using two complementary satellite data sources. The longer-term Landsat series provided observations for 2010 – 2024 with a temporal resolution of 8 – 16 days and Harmonized Landsat Sentinel-2 (HLS) data covered 2015 – 2024 at a higher temporal resolution of 2 – 3 days (Masek et al., 2021). For HLS data, we created composites using maximum NDVI for mid-July through the end of September, which selects the highest value per pixel to capture peak vegetation. For Landsat data, we compared both maximum and minimum compositing techniques over the same time period to evaluate which better captured NDVI changes associated with oak decline. We used this approach to assess the change detection methodology across different sensor characteristics, temporal resolutions, and compositing methods.

We processed environmental data (climate variables, topographical variables, and cropland proximity) and performed temporal NDVI change detection. We also conducted statistical analysis to examine relationships between environmental factors and observed decline. Using weighted overlay analysis, we generated separate mortality risk maps for the Kaskaskia River Basin and Shawnee National Forest to capture region-specific patterns.

3.1 Data Acquisition

We acquired environmental input variables for the risk map from multiple sources: publicly available NASA Earth observations (Table A1), climate data from the Gridded Surface Meteorological (GridMET) dataset, topographic data from the Illinois State Geological Survey, and commercial cropland data from the US Department of Agriculture (USDA) (Table A2). We utilized the US Forest Service's Individual Tree Species Parameter map to acquire white oak stand locations throughout the study areas. Additionally, we used ancillary data provided by the Morton Arboretum, including aerial flight imagery and root sample location points, showing locations of known, declined oak stands (Table A3).

3.1.1 Earth Observations

We acquired HLS data – comprised of Landsat 8 Operational Land Imager (OLI), Landsat 9 OLI-2, Sentinel-2A and Sentinel-2B Multi-Spectral Instrument (MSI) – from the Land Processes Distributed Active Archive Center (LP DAAC) using the NASA Earthdata interface and filtered for summer periods between 2015 and 2024 (July 15th to September 30th) and cloud cover less than 20% for both study regions. HLS combines imagery from sensors aboard Landsat 8, Landsat 9, and Sentinel-2, providing a higher temporal revisit time and improved radiometric correction, which is useful for monitoring rapid changes in vegetation health. The Landsat 8 OLI, Landsat 9 OLI-2, and Sentinel-2 MSI optical sensors are harmonized to produce the HLS surface reflectance product (HLSL30.020), which provides consistent bidirectional reflectance distribution function corrected observations at a 2–3-day temporal resolution and 30-meter spatial resolution (Masek et al., 2021). To acquire this HLS imagery, we used ArcPy, a Python-based spatial analysis module integrated within ArcGIS. We incorporated the "earthaccess" Python library to directly download the satellite imagery. ArcPy enabled efficient processing and analysis across large geographic areas, extending beyond the limitations of using single tile layers that had to be subsequently stitched to represent the study area.

We retrieved Landsat 5 Thematic Mapper (TM), Landsat 7 Enhanced Thematic Mapper Plus (ETM+), Landsat 8 OLI, and Landsat 9 OLI-2 Collection 2 Level 2 data from ArcGIS for Microsoft Planetary Computer within the ArcGIS Pro 3.3 ArcPy interface (Zhan, 2024). ArcGIS for Microsoft Planetary Computer provides direct access to the Microsoft Planetary Computer Data Catalog. We used the Spatio-Temporal Asset Catalog application programming interface to query the Microsoft Planetary Computer data catalog for Collection 2 Level 2 Landsat scenes, within a bounding box of our study area and between the dates of July 15th and September 30th, for scenes with cloud cover less than 20% for every year between 2010 and 2024. However, the years 2013, 2018, 2020, and 2024 were filtered for scenes with cloud cover less than 30% due to higher cloud cover for these summers. We leveraged Landsat-based Detection of Trends in Disturbance and Recovery ("LandTrendr"), an ArcGIS remote sensing tool specifically designed to detect and analyze vegetation changes over time using satellite imagery, to examine annual time series data from both HLS and Landsat imagery, allowing for the detection of disturbance on a vast temporal scale capturing not only large-scale variations but also abrupt, short-term changes. By applying "LandTrendr" to the dataset, we were able to produce detailed timelines of vegetation fluctuations, pinpointing specific years where notable declines in NDVI were detected.

3.1.2 Topographic, Climate, and Commercial Cropland Data

We acquired a 30-meter digital elevation model (DEM) from the Illinois Geospatial Data Clearinghouse (Luman et al., 2003; Table A2). The DEM data used a Transverse Mercator projection with the parameters of UTM Zone 16, NAD27. We derived all other topographic features from this DEM.

We obtained climate data using Climate Engine's Research App, a web-based climate data acquisition interface. Using GridMET data at 4-kilometer spatial resolution (approximately 1,600 hectares or 3,954 acres per pixel), we extracted data from three key variables for each region: total precipitation anomalies (PPT) from 30-year seasonal baseline periods (1994 – 2024), 90-day Standardized Precipitation Index (SPI), and daily maximum temperature averaged over June – August (Table A2). We selected 90-day SPI to provide a seasonal time window for drought assessment across meteorological winter (December – February), spring (March – May), and summer months (June – August), while daily maximum temperatures were selected and averaged specifically for the summer season to investigate how heat stress might affect tree growth during oak trees' primary growing season (Sohar et al., 2013). We retrieved cropland cover data for 2023 from the USDA Cropland Data Layer using the web app CroplandCROS (USDA & National Agricultural Statistics Service, 2023; Table A2). We included all land cover types in this initial extraction, and commercial crops were later filtered out during processing.

3.2 Data Processing

3.2.1 Earth Observations

We processed the HLS dataset using ArcGIS Pro and its ArcPy interface, specifically utilizing the red and near-infrared (NIR) bands across the study area for each summer between 2015 and 2024. Given the extent of the study area, we needed to download multiple image tiles for each band. We then mosaicked these separate tiles into two consolidated images for each summer: one complete image for the red band and one for the NIR band. The red and NIR bands were used to create NDVI composites for each scene (Equation 1; Kriegler et al., 1969) on a per-pixel basis to capture detailed vegetation changes over time for 2015 – 2024. We derived the summer maximum NDVI values for each pixel, allowing a detailed investigation of the health of oak vegetation over the years. We used quality assurance procedures, including cloud and shadow masking, to ensure data accuracy and reliability. This helped to ensure that only high-quality pixels were used in our analysis to improve data accuracy and allow for a more reliable assessment of vegetation trends. We identified changes in NDVI by computing the difference of each pixel's NDVI between the summer of 2023 and summer 2024. This NDVI change map was subsequently clipped to our white oak stands layer with a basal area > 20 sq ft/acre from the 2012 Individual Tree Species Parameter Map, masked for water bodies using the USGS National Hydrography Dataset (United States Geological Survey, National Geospatial Program, 2023), and clipped to a higher resolution deciduous forest layer from the USDA Cropland Data Layer.

$$\mathrm{NDVI} = \frac{\mathrm{NIR} - \mathrm{Red}}{\mathrm{NIR} + \mathrm{Red}} \tag{1}$$

We preprocessed Landsat satellite imagery (Landsat 5 TM, Landsat 7 ETM+, Landsat 8 OLI, and Landsat 9 OLI-2 Collection 2 Level-2 scenes) accessed through the ArcGIS for Microsoft Planetary Computer using the ArcGIS Pro ArcPy interface. We removed clouds and cloud-shadows using the Landsat QA Band and applied a scaling factor and additive offset to the data to convert them from floating point to 16-bit integer format. For each scene, we generated NDVI composites using the red and NIR bands (Equation 1; Kriegler et al., 1969). NDVI composites from each scene from a single summer were then composited together using the minimum or maximum NDVI value for overlapping pixels. As a result, for each summer, we had one cloud-free NDVI composite using the maximum compositing method and one cloud-free NDVI composite using the minimum compositing method. This was conducted for each summer of our study period, resulting in 15 maximum NDVI composites for 2010 – 2014 and 15 minimum NDVI summer composites for 2010 – 2014. Both minimum and maximum compositing techniques were used for pixels with multiple NDVI observations to determine the best apparent method for identifying negative NDVI change in this study area and study period. The resulting composites were converted into two multidimensional time-aware mosaics (one for minimum and one for maximum values. We clipped these mosaics to white oak stands with a basal area >20 sq ft/acre using the 2012 Individual Tree Species Parameter Map. Then, we masked the dataset for water bodies using the USGS National Hydrography Dataset (United States Geological Survey, National Geospatial Program, 2023) and further refined the dataset by clipping it to a higher resolution deciduous forest layer from the USDA Cropland Data Layer.

We used the "Change Detection" toolset within the ArcGIS Pro 3.3 Image Analyst toolbox to map changes in NDVI between each summer and across our study period for both Landsat and HLS datasets. We generated individual 2-date (e.g., summer for current year versus summer for previous year) NDVI change maps using the "Compute Change Raster" tool. We leveraged Landsat-based Detection of Trends in Disturbance and Recovery ("LandTrendr"), an ArcGIS remote sensing tool specifically designed to detect and analyze vegetation changes over time using satellite imagery, to examine annual time series data from both HLS and Landsat imagery, allowing for the detection of disturbance on a vast temporal scale capturing not only large-scale variations but also abrupt, short-term changes. By applying "LandTrendr" to the dataset, we were able to produce detailed timelines of vegetation fluctuations, pinpointing specific years where notable declines in NDVI were detected. Then, we used the clipped and water-masked HLS and Landsat multidimensional-aware mosaics to generate wall-to-wall maps using the "Analyze Changes Using LandTrendr" tool. The output change analysis raster contains model results from the "Analyze Changes Using LandTrendr" tool. These model results describe a set of linear models for the NDVI time series which segments a pixel's time series into periods of change, no change, and recovery from change (Table A4). We input these coefficients into the "Detect Change Using Change Analysis Raster" tool to produce date of change information for every pixel of interest in our study area (Table A4). We then filtered the LandTrendr results to find the largest negative change within the time series with a minimum magnitude of 0.1 to filter out smaller decreases in NDVI.

3.2.2 Topographic Data

We conducted topographic analysis through the SAGA GIS 9.6.1 software and closely followed the Topographic Wetness Index (TWI) workflow of Kopecký et al. (2021). We first filled the 30-meter DEM using the "Fill Sinks XXL" tool to eliminate any erroneous sinks or peaks that may have been present in the raw DEM. The minimum slope was set to 0.01° to prevent dividing by zero during the later TWI calculations. In addition to filling depressions, this tool also preserves the downward slope along a flow path and can process large datasets. The filled DEM served as the input for all subsequent tools, except for the TWI calculation. We produced slope and aspect layers using the "Slope, Aspect, and Curvature" tool, set the unit parameters to radians and degrees, respectively, and set the method parameter to a third-degree polynomial. The Slope (S) layer produced by this step was used for further TWI calculations (Equation 2); the resulting slope and aspect layers were also used as inputs for the risk map. Flow accumulation and width were calculated to support TWI modeling. We used the "Flow Accumulation (Top-Down)" tool because the parameters can be altered to create a multiple-direction flow path, which provides more robust flow accumulation measurements compared to single-direction methods (Kopecký et al., 2021). We set the method and convergence parameters to "Multiple Flow Direction" and 1.1, with the latter representing a moderate flow dispersion value and the resulting layer represented the total catchment area (TCA; Equation 2). We set the method for the "Flow Width and Specific Catchment Area" tool to Multiple Flow Direction and the layer produced represented the Flow Width (FW; Equation 2). To calculate TWI, we input the resulting slope, total catchment area, and flow width layers into the 'Grid Calculator' tool following the equation below from Kopecký et al. (2021) to create the TWI layer.

$$TWI = \ln\left(\frac{\left(\frac{TCA}{FW}\right)}{\tan(S)}\right) \quad (2)$$

3.2.3 Climate Data

The precipitation and SPI variables were temporally filtered to cover the study period. In choosing seasonal timeframes, we followed the meteorological definition of seasons that allows seasonal comparisons across climatological studies. We filtered precipitation and SPI data for winters (December, January, February), springs (March, April, May), and summers (June, July, August) between 2009 and 2024. Daily maximum

temperatures were averaged for meteorological summers. We performed data processing in R 2024.04.0 using the "tidyverse" suite for data manipulation, while the packages "terra" and "sf" were employed for handling raster data and vector shapefiles, respectively. To support the Morton Arboretum in investigating potential climatic relationships with oomycete presence, which may contribute to oak wilt, we visualized winter and spring conditions using paired time series plots created with ggplot2. These plots display SPI values for winter and spring seasons side-by-side for each year of the study period.

3.2.4 Cropland Data

From the USDA Cropland Data Layer, we extracted specific commodity crops using the "Select by Attribute" tool. Following our partner's guidance, we excluded agricultural landcovers unlikely to receive herbicide applications, such as hay and pasture (Table A5), to better assess the potential impacts of herbicide drift. We also calculated the proximity of oak stands to agricultural stands by using the "Euclidean Distance" tool in ArcGIS Pro. Then, we input the agricultural raster layer into the tool, which created a raster surface of distances emanating from crop cells that was later used in the decline risk mapping. This raster layer was clipped to the white oak stand extent to create a surface of proximity values to crops for visualization.

3.3 Data Analysis

3.3.1 Assessing Drivers of Change Across Study Areas

The Kaskaskia River Basin and Shawnee National Forest differ substantially in land cover composition, environmental conditions, and land management practices, necessitating separate risk analyses for each region. To identify key drivers of white oak mortality risk and determine their relative importance, we conducted independent analyses for each study area. This approach combined a principal component analysis (PCA) with a risk classification scheme to create regional risk maps. We began by using white oak stand boundaries (a combined polygon of white oak stands with basal area >20 sq ft/acre and known oak decline areas provided by the partner) to mask out all non-oak stand areas, then converted all input raster datasets to tabular form in R.

We employed the PCA to identify the key drivers of environmental variation across white oak stands, with the selected input variables of NDVI change between the summers of 2023 and 2024 from Landsat minimum composites, proximity to commercial croplands, TWI, slope, northness, eastness, average summer maximum temperature for 2024, and average summer drought SPI for 2024. Prior to conducting the PCA, we preprocessed the input variables to remove all NA values, as well as normalized to achieve distributional consistency. Crop proximity data and TWI were square root transformed, and aspect was separated into "northness" and "eastness" components using the cosine and sine of the aspect, respectively. After the normalization, a z-score standardization was applied to achieve constancy across scale.

The PCA helped us determine the relative importance of each variable by measuring how much it contributed to the overall variation in site conditions. While NDVI change was included in the PCA to understand the relationship between it and other environmental variables, we excluded it from the final risk mapping to avoid circularity since NDVI change itself is an indicator of decline. For the Shawnee National Forest analysis, we excluded cropland proximity data per the Morton Arboretum's suggestion since cropland is a less major component of land use in Shawnee National Forest as in Kaskaskia. We worked with the partner to develop a risk classification scheme for each variable that reflected both ecological understanding and management priorities. These classification schemes were combined with the PCA-derived weights to generate weighted overlay risk maps. This approach leverages both statistical relationships in the data and on-the-ground expertise – particularly valuable given the emerging nature of white oak decline research, where the complex interactions between risk factors are still being understood.

3.3.2 Creating a White Oak Mortality Risk Map

After deriving variable weights through statistical analyses, we developed mortality risk maps for each study area using ArcGIS Pro geoprocessing tools. First, we ranked each input variable using the "Reclassify" tool on a common scale of 1 – 5, where higher values represent conditions more conducive to mortality risk. We

used a mixture of literature, expert advice, and team discretion to derive value rankings for each variable (Rogers, n.d.; Table A7). This reclassification process translated the raw data into comparable risk scores. We then integrated the reclassified variables using the "Weighted Overlay Analysis" tool, applying the derived weights specific to each study area (Table A7). This weighted overlay process combined our input variables into a single composite risk surface, where each cell's final value represents the relative risk based on each variable's importance (determined by PCA-derived weights). We produced separate risk maps for the Kaskaskia River Basin and Shawnee National Forest, with each map reflecting the uninque relationships between environmental conditions and mortality risk specific to its region.

4. Results

4.1 Analysis of Results

4.1.1 Detecting changes in oak tree health through Earth observations

We examined recent vegetation changes in known oak stands by comparing 2023 – 2024 NDVI change maps using HLS and Landsat data minimum and maximum compositing. This change detection technique offered a spatially detailed view of where and to what extent vegetation had fluctuated in the Shawnee National Forest and Kaskaskia River Basin. Areas exhibiting significant decline were in the eastern, central, and northwest parts of Shawnee National Forest as well as the southeastern border of Kaskaskia (Figure B1). The Landsat minimum compositing NDVI change map for 2023 – 2024 successfully identified decreases in NDVI in areas of known oak decline (Figure B1; Figure B2; United States Forest Service, 2024). The inability of HLS maximum (Figure B2) and Landsat maximum compositing to identify decreases in NDVI is likely due to pre-disturbance NDVI values concealing the lower post-disturbance NDVI values from later in the compositing window.

We identified previous decreases in the vegetation greenness of white oak stands between 2010 and 2024 using LandTrendr minimum compositing Landsat data (Figure B5) and maximum compositing HLS data (Figure B8). LandTrendr allowed for wall-to-wall disturbance mapping and identified decreases in NDVI throughout our study period, though the vast majority of changed pixels were in summer of 2024 (Figure B3) This is likely due to the parameters chosen to run LandTrendr, which specifically focused on the date at the end of segment for the largest change in the pixel's timeseries (Table A4). Our conservative spike threshold of 0.75 aggressively dampened anomalies in a pixel's NDVI trajectory, though could lead to errors of omission in the results (Figure B4). Decreases in NDVI detected by the LandTrendr algorithm for 2024 were visually compared with 2023 – 2024 NDVI Landsat minimum compositing change map (Figure B5). The LandTrendr algorithm detected more changed pixels compared to the 2023 – 2024 NDVI change for the growing season in 2024. This could be due to the less aggressive filtering of the LandTrendr results to include only changes with a minimum magnitude greater than 0.1 (Table A4). Future studies should continue to iteratively explore the minimum magnitude parameter to determine the most suitable level of filtering.

4.1.2 Assessing potential risk variables and their relationships to decline in white oak health

Precipitation patterns in the Shawnee National Forest and Kaskaskia regions exhibited distinct temporal characteristics from 2010 to 2024. The Kaskaskia region demonstrated a recurring dry-winter-wet-spring pattern in at least six out of fourteen years (2010 – 2011, 2012 – 2013, 2014 – 2015, 2016 – 2017, 2017 – 2018, and 2018 – 2019), with three additional years showing localized expressions of the pattern (2019 – 2020, 2020 – 2021, 2021 – 2022). In comparison, Shawnee National Forest displayed dry-winter-wet-spring less frequently, only in three years of the study period (2010 – 2011, 2014 – 2015, and 2016 – 2017). Since winter 2019, both regions have experienced predominantly negative precipitation anomalies, though some localized areas in Kaskaskia maintained dry-winter-wet-spring. Summer precipitation patterns showed similar trajectories in both regions, with sustained negative anomalies during 2010 – 2014, followed by wetter conditions in 2015 – 2016 (mixed conditions in Kaskaskia). The year 2017 marked a severe drought across both regions. The period of 2018 – 2024 was characterized by predominantly dry conditions, with some temporal variability. In the SPI data, which quantifies precipitation deficits at individual pixels rather than regional averages, Kaskaskia showed dry-winter-wet-spring during 2010 – 2011, 2017 – 2018, and 2021 – 2022, while Shawnee exhibited this pattern during 2010 – 2011, 2014 – 2015, 2015 – 2016, and 2017 – 2018.

Severe summer drought stress affected Shawnee in seven years (2010, 2012, 2013, 2017, 2021, 2022, and 2024) while Kaskaskia experienced drought stress in eight years (2011, 2012, 2013, 2017, 2018, 2019, 2022, 2023). Average summer maximum temperatures ranged from 32°C to 47°C throughout the study period for both study areas. The warmest conditions occurred during 2010 – 2013, with 2012 experiencing particularly high maximum temperatures exceeding forty degrees in both regions. While the period from 2014 – 2020 showed no significant average summer maximum temperature anomalies, 2021 – 2024 exhibited elevated temperatures, though not reaching the intensity observed during 2010 – 2013.

Analysis of topographic features and agricultural proximity revealed distinct landscape characteristics of white oak stands across both regions. While both areas showed right-skewed slope distributions with maximums up to 62 degrees, Shawnee's average slope (26 degrees) was notably steeper than Kaskaskia's (13 degrees). TWI values were comparable, though Kaskaskia showed slightly higher moisture potential with an average TWI of 6.9 compared to Shawnee's 5.8. Oak stands in both regions exhibited a preference for south-facing slopes, with stands distributed relatively evenly between east and west aspects. In Kaskaskia, proximity to commercial cropland showed a right-skewed distribution, with stands ranging from 0 to 3,507 meters from commercial croplands (median: 775m, mean: 889m), indicating a higher frequency of stands closer to croplands.

The PCA results based on Landsat-derived data (minimum NDVI compositing) indicate that slope, TWI, and climate conditions were the primary drivers of variance in both study regions (Table A6). The three principal components explained approximately 47% of the variance in Kaskaskia (19.9%, 15.0%, 12.6%) and 55% in the Shawnee National Forest (22.7%, 17.9%, 14.9%). In both regions, TWI, slope, and climate conditions (drought and average maximum temperature) emerged as the strongest contributing variables. In Kaskaskia, slope showed the highest loading (~36%) followed by TWI (~34%) and SPI (~17%). In the Shawnee National Forest, where crop proximity was not included, slope also showed the highest loading at approximately 25%, followed by TWI (~20%) and average maximum summer temperature (19%). Aspect-related variables differed between the study areas; aspect had a much smaller effect in the Kaskaskia River Basin (eastness 5%, northness 1%) where the terrain is significantly less topographically diverse relative to the Shawnee National Forest (eastness 12%, northness 12%). Similar PCA analyses were conducted using HLS-derived data with maximum compositing, showing slightly different patterns in variable importance – notably more evenly distributed loadings and a stronger influence of climate variables compared to Landsat (Table A6).

4.1.3 Decline Risk Assessment & Mapping

The risk map (Figure B9) revealed oak stand areas with moderate-high to high risk for health decline. The weighting structure of this map followed the Landsat (minimum NDVI compositing) PCA results due to the relatively increased ability of this dataset to capture NDVI change, particularly in areas of known decline. Moderate-high (4) to high-risk (5) values correlate to areas where many or all of the climatic and topographic variables considered are unfavorable conditions for white oak trees. Similarly, low (1), moderate-low (2), and moderate (3) values indicate areas where the environment is more suitable for white oaks. For both study areas, the average risk value was near 3, corresponding to moderate risk; however, the Shawnee National Forest had a slightly higher average risk value of approximately 3 (Figure B6) compared to Kaskaskia, with an average risk value of roughly 2.7 (Figure B7). The distribution of moderate-high to high-risk values for Kaskaskia is more widespread throughout the region. In contrast, more pronounced clusters of these higher-risk categories emerge in the northwestern tip and eastern half of the Shawnee National Forest.

4.2 Errors & Uncertainties

Several key data quality and validation challenges impacted our analysis. While valuable for oak stand identification, the Individual Tree Species Parameter Map introduced uncertainty as an inferenced model. Limited ground-truth examples of white oak decline significantly constrained our ability to validate change detection through unbiased accuracy assessment (Olofsson et al., 2014). This validation gap leaves several questions unanswered: we could not definitively confirm whether areas showing significant NDVI decreases

represent actual white oak mortality versus other oak species or disturbances (e.g., forest fires, logging), verify decline severity, or assess false positive/negative rates. Similarly, our risk modeling approach relied largely on conceptual frameworks due to the scarcity of field observations.

Satellite data processing presented multiple challenges. Due to the multi-month compositing window, maximum NDVI compositing may inadvertently filter out important decline signals during summer periods, while cloud cover and imperfect masking could artificially lower NDVI values. The transition between Landsat (earlier years) and HLS (later years) datasets, combined with Landsat's lower temporal resolution and gaps in cloud-free scenes (notably in 2012), potentially affected our change detection consistency. The change maps and LandTrendr analysis may not fully capture sub-pixel disturbances and would benefit from formal quantitative accuracy assessments.

Additionally, our risk assessment framework contains several sources of uncertainty. TWI, while based on established literature, was not compared to soil moisture data due to time constraints. This omission, combined with inherent DEM resolution effects, may introduce inaccuracies in topographic risk assessment. The herbicide pollution component was necessarily generalized due to limited information on chemical dynamics and application methods, particularly affecting risk assessment in the Kaskaskia River Basin. Additionally, the PCA-derived weighting scheme, while unbiased, may not accurately reflect true risk factors, especially given the incomplete understanding of rapid white oak mortality drivers in the study area.

5. Conclusions

5.1 Interpretation of Results

Our analysis of climate variables, topographic variables, and crop distance revealed several key patterns. Both regions experienced synchronized extreme events, with Kaskaskia showing more frequent dry winter-wet spring patterns on the regional scale. A shift toward predominantly lower precipitation began in 2019, and the period 2010 – 2013 stands out as being particularly warm and dry. The year 2017 emerged as a significant drought year across both regions. The SPI analysis revealed local variations in drought patterns that were not captured by regional precipitation averages. While precipitation anomalies show overall drier conditions since 2019, the 90-day SPI indicates increased winter wetness during 2019 – 2023 with severe drought stress in localized regions. Many of these patterns confirm the partner's original observations of broader climatic trends while providing finer-scale temporal and spatial variations that add critical local context. Additionally, while the TWI mainly served as an input for the decline risk map, the stand-alone TWI map can also assist in identifying areas where oak stands may be inundated with water following precipitation events. TWI value ranges are not fixed like other indices as the resulting values can vary due to the topographic profile of a region and the resolution of the DEM used (Ballerine, 2017). However, regardless of the range, larger values correspond to higher water catchment and pooling compared to lower values, which indicate areas where water largely flows off the surface.

HLS LandTrendr data revealed major negative changes in maximum NDVI between 2021 to 2024 for the Shawnee National Forest and Kaskaskia (Figure B8) which aligns with precipitation anomalies that detected drier conditions since 2019, as well as the temperature data that showed overall elevated temperatures between 2021 and 2024. Certain topographic characteristics also coincided with HLS maximum forest NDVI data that appeared to be associated with observed vegetation greenness decline. Steeper slopes in Shawnee National Forest (5.95 degrees average) promote water runoff which limits soil moisture availability leading to the overall decline in oak tree health. This was evident in the 2023 – 2024 change map as most of the NDVI decline was detected in Shawnee National Forest. In Kaskaskia, the proximity of white oak stands to commercial croplands, with an average of 889 meters, also was associated with forest NDVI decline. This analysis revealed lower NDVI values in oak stands along the Kaskaskia River suggesting a possible relationship between oak health and environmental stressors such as soil moisture variability, herbicide drift and drought frequency in the region.

Regarding the oak decline risk map, several areas of potential conservation concern emerged, particularly in the Shawnee National Forest. In the Kaskaskia River Basin, moderate-high to high-risk values were found scattered throughout the oak stands in this area; no obvious patterns of decline emerged on a large scale. However, on a smaller scale, areas of moderate-high to high risk appeared to follow a web-like pattern potentially related to differences in slope around drainages, but more investigation would be necessary to determine this (Figure 2, upper left inset map). In the Shawnee National Forest, several larger clusters of moderate-high to high risk can be seen, namely the northwestern tip and the eastern half of the study area (Figure 2, lower right inset map). These clusters may be considered when prioritizing areas for future sampling efforts.

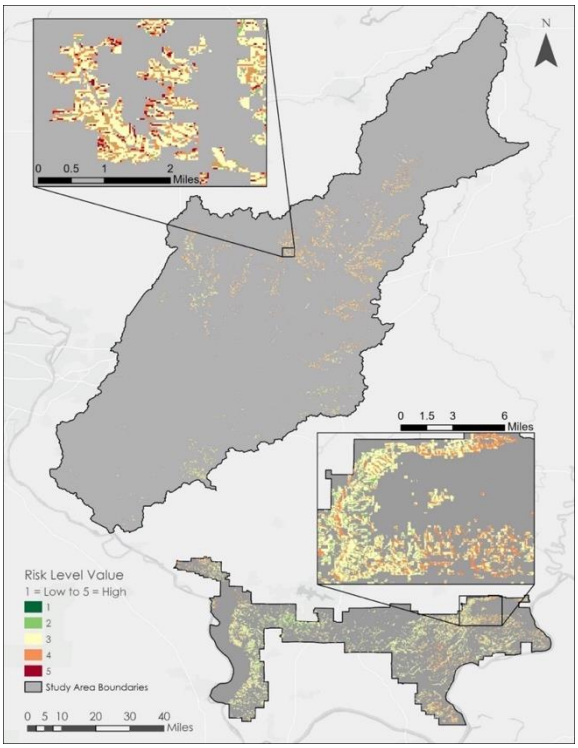

[Basemap CreditsMissouri DNR, Esri, TomTom, Garmin, FAO, NOAA, USGS, EPA, USFWS]

Figure 2. Oak decline risk map of the Kaskaskia River Basin and Shawnee National Forest using PCA values calculated based on Landsat minimum NDVI compositing data. Green shades correlate to areas of low or low-moderate risk (1-2), the light-yellow shade matches areas of moderate risk (3), and the red shades correspond to areas of moderate-high to high risk (4-5). The inset maps highlight areas and patterns of decline.

5.2 Feasibility & Partner Implementation

Overall, this study produced several end products that could be useful to the Morton Arboretum, each with varying degrees of feasibility when it comes to their implementation. The precipitation and drought time series visualizations can be used to locate areas of accumulated climate stress and further examine the hypothesis of dry winters and wet springs potentially leading to increased risk for oomycete invasion. This temporal and spatial analysis of climate-related oak stressors provides data that our partner can refer to when planning future oak sampling efforts. Areas that exhibit the dry winter-wet spring phenomenon, as defined by these maps, may be used to test whether these conditions favor oomycete invasion and abundance through pathogen testing by the partner. This is particularly true for the southern range of Kaskaskia, where oak decline is less studied in the field. However, given the 4-kilometer resolution of the climate data used in this study, the partner may need to implement finer resolution climate data to further pinpoint areas with climatic stress. Similarly, the TWI map can be used to identify more specific areas where water may pool on the

surface and inundate oaks with moisture, creating potentially favorable conditions for oomycetes to thrive (Figure B10).

The Morton Arboretum can also utilize the decline risk map to target areas of sampling and conservation priority, albeit with an understanding that the accuracy of the information on this map is unknown. The risk map draws primarily on conceptual understanding of oak decline patterns and drivers, as limited field data was available for validation. Similarly, the accuracy of the NDVI change maps is also influenced by the lack of in situ and other reference data to compare to. However, these maps provide a general representation of where oaks in the study area may be at risk and where decline may already be occurring, many of which are outside of the currently sampled areas. Therefore, the partner may consider these maps when delineating where to expand their field surveys and sampling efforts. To increase the accuracy of this study, more ground-truth field data would be useful to compile revised models that better depict the reality of this phenomenon.

Future research should utilize the minimum compositing technique with higher temporal resolution HLS data for the creation of seasonal composites used in change analysis. Furthermore, higher temporal resolution data, like HLS (when available), could be useful for continuous change detection and classification analysis to better identify rapid white oak mortality at the intraseasonal level. Nevertheless, it is evident through the Landsat LandTrendr analysis that NDVI declines occurred prior to when HLS data became available in 2015; and therefore, historical analysis of vegetation changes prior to 2015 should utilize Landsat data. In addition, higher spatial resolution (10 meters) Sentinel-2 MSI data could further bolster NDVI change results by picking up on the more nuanced changes in vegetation health. Other vegetation indices, such as the Enhanced Vegetation Index 2 or Normalized Difference Fraction Index, could also be used to detect more subtle vegetation health changes or sub-pixel canopy disturbances, respectively.

The crop proximity map may also be useful to our partner when investigating the impact of herbicide drift pollution on oak decline. While this study did not heavily explore or discuss the relationship between these two factors, the proximity map provides a reference that may be used by the partner to conduct further studies. During field sampling efforts, the partner may use this map to record the approximate distance to nearby cropland and potentially derive a relationship between oak decline and herbicide drift.

6. Acknowledgements

The Illinois Ecological Conservation team thanks our partner point of contact, Dr. Fredric Miller from the Morton Arboretum. We are grateful to Sean McCartney, Joseph Spruce, and Dr. Kenton Ross for advising this project. We would also like to show appreciation to our node lead Isabel Lubitz for her support, as well as Marisa Smedsrud for her guidance on project deliverables.

Any opinions, findings, and conclusions or recommendations expressed in this material are those of the author(s) and do not necessarily reflect the views of the National Aeronautics and Space Administration.

This material is based upon work supported by NASA through contract 80LARC23FA024.

7. Glossary

Basal Area – a measurement of the cross-sectional area of trees at breast height, which is 4.5 feet above the ground
Change detection – a GIS technique used to identify, analyze, and quantify differences in a specific area over time
Earth observations – satellites and sensors that collect information about the Earth's physical, chemical, and biological systems over space and time
HLS – Harmonized Landsat and Sentinel-2, a dataset that combines observations from multiple satellite systems (Landsat and Sentinel-2) to provide high temporal resolution Earth observation data (2 – 3 days)

Landsat – a series of Earth observing satellite missions jointly managed by NASA and the USGS that collects images of the Earth's surface to study the planet and its changes
LandTrendr – a remote sensing tool specifically designed to detect and analyze vegetation changes over time using satellite imagery
Maximum compositing – a technique used to create cloud-free vegetation (like NDVI) by selecting the highest value for each pixel from a series of observations over a specific time period (typically 8-16 days); This method helps reduce the effects of clouds, atmospheric interference, and viewing angle variations while capturing peak vegetation conditions, since clouds and atmospheric effects typically lower NDVI values
Minimum compositing – a technique that selects the lowest value for each pixel from a series of temporal observations; While less commonly used than maximum compositing for vegetation studies (since low NDVI values often represent cloud contamination), minimum compositing can be valuable for detecting vegetation stress, senescence, or die-off events since it captures the most severe decline in vegetation condition during the compositing period
NDVI – Normalized Difference Vegetation Index, a measurement that uses visible and near-infrared light reflected by vegetation to assess plant health and density
PCA – principal component analysis, a statistical technique used to reduce the dimensionality of large datasets while preserving important patterns and relationships
Rapid White Oak Mortality – a condition characterized by the sudden and unexpected decline of white oak trees
SAGA GIS – a geospatial information system software used to edit, manipulate, and analyze geospatial data
SPI – Standardized Precipitation Index, a widely used index to characterize meteorological drought on various timescales
TWI – Topographical Wetness Index, a steady-state wetness index that describes the tendency of water to accumulate at any point in a watershed
White Oak decline – a condition that affects oak trees and is characterized by yellowing or browning of leaves, thinning of the canopy and sprouts on the trunks
Weighted Overlay – a GIS technique used to combine multiple layers of spatial data by assigning each layer a weight based on its importance in the analysis

8. References

Aubard, V., Paulo, J. A., & Silva, J. M. N. (2019). Long-term monitoring of cork and holm oak stands productivity in Portugal with Landsat imagery. *Remote Sensing, 11*(5), 525. https://doi.org/10.3390/rs11050525

Ballerine, C. (2017). *Topographic Wetness Index Urban Flooding Awareness Act Action Support: Will and DuPage Counties, Illinois.* (Contract Report 2017(02)). Illinois State Water Survey, Prairie Research Institute, University of Illinois. https://www.isws.illinois.edu/pubdoc/CR/ISWSCR2017-02.pdf

Catalão, J., Navarro, A., & Calvão, J. (2022). Mapping cork oak mortality using multitemporal high-resolution satellite imagery. *Remote Sensing, 14(*12), 2750. https://doi.org/10.3390/rs14122750

Crocker, E., Gurung, K., Calvert, J., Nelson, C. D., & Yang, J. (2023). Integrating GIS, remote sensing, and citizen science to map oak decline risk across the Daniel Boone National Forest. *Remote Sensing*, *15*(9), 2250. https://doi.org/10.3390/rs15092250

Earth Resources Observation and Science (EROS) Center. (2020). *Landsat 8-9 Operational Land Imager / Thermal Infrared Sensor Level-2, Collection 2* [dataset]. United States Geological Survey. https://doi.org/10.5066/P9OGBGM6

Earth Resources Observation and Science (EROS) Center. (2020). *Landsat 7 Enhanced Thematic Mapper Plus Level-2, Collection 2* [dataset]. US Geological Survey. https://doi.org/10.5066/P9C7I13B

Earth Resources Observation and Science (EROS) Center. (2020). *Landsat 4-5 Thematic Mapper Level-2, Collection 2* [dataset]. US Geological Survey. https://doi.org/10.5066/P9IAXOVV.

El Ahmadi, S., Ramzi, H., Aafi, A., Jmii, N. E., & Aadel, T. (2023). Assessment of cork oak decline using digital multispectral imagery in relation with in situ crown condition. *Open Journal of Forestry, 13*, 145 – 160. https://doi.org/10.4236/ojf.2023.131010

Hwang, K., Harpold, A. A., Tague, C. L., Lowman, L., Gabrielle, Lininger, K. B., Sullivan, P. L., Manning, A., Graup, L., Litvak, M., Lewis, G., Miller, K., Brooks, P. D., & Barnard, H. R. (2023). Seeing the disturbed forest for the trees: Remote sensing is underutilized to quantify critical zone response to unprecedented disturbance. *Earth's Future*, *11*(8). https://doi.org/10.1029/2022ef003314

Illinois Department of Natural Resources. (2017). *Illinois forest action plan: A statewide forest resource assessment and strategy* (Version 4.0). https://dnr.illinois.gov/content/dam/soi/en/web/dnr/conservation/forestry/urbanforestry/documents/illinois-statewide-forest-resource-assessment-sand-strategies4-0.pdf

Illinois Department of Natural Resources. (n.d.). *Kaskaskia River.* I Fish Illinois. https://www.ifishillinois.org/profiles/Kaskaskia.php

Infrastructure Investment and Jobs Act, 23 U.S.C. § 101 et seq. (2021). https://www.congress.gov/bill/117thcongress/house-bill/3684/text

Kamoun, S., Furzer, O., Jones, J. D. G., Judelson, H. S., Ali, G. S., Dalio, R. J. D., Roy, S. G., Schena, L., Zambounis, A., Panabières, F., Cahill, D., Ruocco, M., Figueiredo, A., Chen, X.-R., Hulvey, J., Stam, R., Lamour, K., Gijzen, M., Tyler, B. M., & Grünwald, N. J. (2014). The top 10 oomycete pathogens in molecular plant pathology. *Molecular Plant Pathology, 16*(4), 413–434. https://doi.org/10.1111/mpp.12190

Kennedy, R. E., Yang, Z., & Cohen, W. B. (2010). Detecting trends in forest disturbance and recovery using yearly Landsat time series: 1. LandTrendr—Temporal segmentation algorithms. *Remote Sensing of Environment*, *114*(12), 2897-2910. https://doi.org/10.1016/j.rse.2010.07.008

Knoot, T. G., Shea, M. E., Schulte, L. A., Tyndall, J. C., Nelson, M. D., Perry, C. H., Palik, B. J. (2015). Forest change in the Driftless Area of the Midwest: From a preferred to undesirable future. *Forest Ecology and Management, 341*, 110-120. http://dx.doi.org/10.1016/j.foreco.2014.12.013

Kopecký, M., Macek, M., Wild, J. (2021). Topographic Wetness Index calculation guidelines based on measured soil moisture and plant species composition. *Science of Total Environment, 757*, 143785. https://doi.org/10.1016/j.scitotenv.2020.143785

Kriegler, F., Malila, W., Nalepka, R., & Richardson, W. (1969). Preprocessing transformations and their effect on multispectral recognition. *Proceedings of the 6th International Symposium on Remote Sensing of Environment. University of Michigan, Ann Arbor*, 97-131.

Krohe, J., Jr. (2001). *The Kaskaskia River Basin: An inventory of the region's resources*. Illinois Department of Natural Resources. https://www.ideals.illinois.edu/items/14456

Luman, D., Smith, L., Goldsmith, C. (2003). *Illinois Statewide 30-Meter Digital Elevation Model* (Edition 1) [Data Set]. Illinois State Geological Survey. https://clearinghouse.isgs.illinois.edu/data/elevation/surface-elevation-30-meter-digital-elevation-model-dem

Macháčová, M., Nakládal, O., Samek, M., Bať a, D., Zumr, V., & Pešková, V. (2022). Oak decline caused by biotic and abiotic factors in Central Europe: A case study from the Czech Republic. *Forests, 13*(8), 1223. https://doi.org/10.3390/f13081223

Masek, J., Ju, J., Roger, J., Skakun, S., Vermote, E., Claverie, M., Dungan, J., Yin, Z., Freitag, B., & Justice, C. (2021). *HLS Operational Land Imager Surface Reflectance and TOA Brightness Daily Global 30m v2.0 – HLSL30.002* [Data set]. NASA EOSDIS Land Processes DAAC. https://doi.org/10.5067/HLS/HLSL30.002

Miller, F. (2024). Aerial survey imagery of oak decline in the Shawnee National Forest [Unpublished photographs].

Miller, F., & Rayfield, C. (2024). Oomycete oak root sampling [Unpublished raw data]. The Morton Arboretum.

Novick, K. A., Jo, I., D'Orangeville, L., Benson, M., Au, T. F., Barnes, M. L., Denham, S. O., Fei, S., Heilman, K., Hwang, T., Keyser, T. L., Maxwell, J. T., Miniat, C. F., McLachlan, J. S., Pederson, N., Wang, L., Wood, J. D., & Phillips, R. P. (2022). The drought response of Eastern US Oaks in the context of their declining abundance. *BioScience, 72*(4), 333–346. https://doi.org/10.1093/biosci/biab135

Olofsson, P., Foody, G. M., Herold, M., Stehman, S. V., Woodcock, C. E., & Wulder, M. A. (2014). Good practices for estimating area and assessing accuracy of land change. *Remote sensing of Environment*, *148*, 42-57. https://doi.org/10.1016/j.rse.2014.02.015

Pascual, L. S., Segarra-Medina, C., Gómez-Cadenas, A., López-Climent, M. F., Vives-Peris, V., & Zandalinas, S. I. (2022). Climate change-associated multifactorial stress combination: A present challenge for our ecosystems. *Journal of Plant Physiology, 276,* 153764. https://doi.org/10.1016/j.jplph.2022.153764

Rogers, R. (n.d.). *White Oak.* United States Department of Agriculture Forest Service. https://www.srs.fs.usda.gov/pubs/misc/ag_654/volume_2/quercus/alba.htm

Sapes, G., Lapadat, C., Schweiger, A. K., Juzwik, J., Montgomery, R., Gholizadeh, H., Townsend, P. A., Gamon, J. A., & Cavender-Bares, J. (2022). Canopy spectral reflectance detects oak wilt at the landscape scale using phylogenetic discrimination. *Remote Sensing of Environment, 273,* 112961. https://doi.org/10.1016/j.rse.2022.112961

United States Department of Agriculture & National Agricultural Statistics Service. (2023). *2023 Illinois Cropland Data Layer* (2023 Edition) [Data Set]. USDA NASS CroplandCROS. https://croplandcros.scinet.usda.gov/

United States Geological Survey, National Geospatial Program. (2023). *USGS National Hydrography Dataset Best Resolution (NHD) for Hydrological Unit (HU) 4 - 0514 Shapefile* [Dataset]. United States Geological Survey. https://www.sciencebase.gov/catalog/item/61f8ba28d34e622189c32c24

United States Forest Service. (2012). *Individual Tree Species Parameter Maps* [Data Set]. United States Department of Agriculture Forest Service. https://www.fs.usda.gov/science-technology/data-tools-products/fhp-mapping-reporting/individual-tree-species-parameter-maps

United States Forest Service. (n.d. -a). *About the Shawnee National Forest.* United States Department of Agriculture. https://www.fs.usda.gov/main/shawnee/about-forest

United States Forest Service. (n.d. -b). *Natural areas of the Shawnee National Forest.* US Department of Agriculture. https://www.fs.usda.gov/Internet/FSE_DOCUMENTS/fseprd575423.pdf

United States Forest Service. (2024). Oak decline surveys in Shawnee & Hoosier National Forest [Unpublished report].

Zhan, S. (2024). ArcGIS for Microsoft Planetary Computer (ArcGIS Pro 3.3). [Notebook Examples]. https://github.com/Esri/arcgis-for-mpc/tree/main

9. Appendices

Appendix A: *Earth Observation, Topographic, Climate, Cropland Datasets and Analytical Methods for White Oak Mortality Assessment Including Change Detection Parameters, Principal Component Analysis, and Variable Classification and Weighting*

Table A1
NASA Earth Observations Utilized to derive NDVI Change in known White Oak stands

Earth Observation Product	Level	Spatial Resolution	Temporal Resolution	Project Use	Temporal Coverage
Landsat 5 Thematic Mapper (TM)	Level 2	30m	16 days	Deriving NDVI change	2010 – 2012
Landsat 7 Enhanced Thematic Mapper Plus (ETM+)	Level 2	30m	16 days	Deriving NDVI change	2012
Landsat 8 Operational Land Imager (OLI)	Level 2	30m	16 days	Deriving NDVI change	2013 – 2024
Landsat 9 Operational Land Imager-2 (OLI-2)	Level 2	30m	16 days	Deriving NDVI change	2022 – 2024
HLSL30.020	Level 2	30m	2-3 days	Deriving NDVI change	2015 – 2024

Table A2
Topographic, Climate, and Commercial Cropland Data organized by the parameters of interest and their source, level, resolution, use, and temporal coverage

Parameter	Source	Level	Spatial Resolution	Project Use	Temporal Coverage
Cropland Data	USDA Cropland Data Layer	Level 4	30m	Deriving oak stand distance to commercial croplands	2023
DEM	ISGS GIS Database	Level 2	30m	Deriving topographical variables	2003
Daily Total Precipitation (mm)	GridMET	Level 4	4km	Time Series Visualizations and Risk Model Input	2010 – 2024
90-day SPI	GridMET	Level 4	4km	Time Series Visualizations and Risk Model Input	2010 – 2024
Daily Maximum Temperature averaged over the summer season	GridMET	Level 4	4km	Time Series Visualizations and Risk Model Input	2010 – 2024

Table A3
Ancillary Data for Assessing Risk Factors on White Oak Mortality

Parameter	Source	Level	Spatial Resolution	Project Use	Dataset Year
Cropland Data	USDA Cropland Data Layer	Level 4	30m	Deriving oak stand distance to commercial croplands	2023
DEM	ISGS GIS Database	Level 2	30m	Deriving topographical variables	2003
White Oak Stands (>20 sq ft/ acre)	US Forest Service Individual Tree Species Parameter Maps	Level 4	30m	Identifying white oak stands	2012
Known Oak Decline Maps	Partner Provided	N/A	N/A	Identifying white oak stands	2024
Oomycete Presence Root Sampling Data	Partner Provided	N/A	N/A	Identifying white oak stands	2023, 2024
Non-Forest Cover Type	USGS Watershed Boundaries Dataset	Level 4	10m	Masking out non-forested areas i.e. hydrological layers	2023
Aerial Imagery of Shawnee National Forest	Partner Provided	N/A	N/A	Identifying white oak stands	2024

* Not directly applied in vegetation change detection analysis or risk map.

Table A4
Configuration parameters used for vegetation change analysis: LandTrendr (left) and Change Analysis Raster settings (right)

Parameter	Value	Parameter	Value
snapping_date	07/15	change_type	TIME_OF_LARGEST_CHANGE
max_number_segments	5	max_number_changes	1
vertex_count_overshoot	2	segment_date	END_OF_SEGMENT
spike_threshold	0.75	change_direction	DECREASE
recovery_threshold	0.25	min_magnitude	0.1
prevent_one_year_recovery	true		

recovery_trend	true		
min_num_observations	6		
best_model_proportion	1.25		
pvalue_threshold	0.01		

Table A5
USDA cropland types categorized by use

Category	Type
Crops of Interest	Corn, rice, sorghum, soybeans, sunflower, sweet corn, pop or orn corn, winter wheat, rye, oats, potatoes, miscellaneous vegetables and fruits, peas, herbs, sod/grass seed, peaches, apples, Christmas trees, pecans, walnuts, pumpkins, cabbage, and double/mixed crop types
Unrelated to Herbicide	Alfalfa, other hay/non-alfalfa, clover/wildflower, grassland/pasture, forest types, shrubland, barren, fallow/idle cropland, water, wetlands, developed types

Table A6
PCA results

Dataset	Min or Max NDVI	Region	Final weighted loadings	Proportion of variance explained by first 3 PCs*	Notes
HLS	Max	Kaskaskia	crop_proximity 0.146 TWI 0.165 slope 0.180 SPI_2024 0.157 max_summer_temp_2024 0.124 eastness 0.090 northness 0.139	PC1: 0.201 PC2: 0.178 PC3: 0.126	Applied log to transform slope
HLS	Max	Shawnee National Forest	TWI 0.208 slope 0.209 SPI_2024 0.227 max_summer_temp_2024 0.190 eastness 0.052 northness 0.114	PC1: 0.219 PC2: 0.167 PC3: 0.154	No cropland layer in PCA
Landsat 5, 7, 8, 9	Max	Kaskaskia	crop_proximity 0.060 TWI 0.341 slope 0.357 SPI_2024 0.173 max_summer_temp_2024 0.007 eastness 0.052 northness 0.010	PC1 0.198 PC2 0.153 PC3 0.130	Applied log to transform slope
Landsat 5, 7, 8, 9	Min	Kaskaskia	crop_proximity 0.064 TWI 0.343 slope 0.358 SPI_2024 0.169 max_summer_temp_2024 0.005	PC1: 0.199 PC2: 0.150 PC3: 0.126	Applied log to transform slope

			eastness 0.051 northness 0.010		
Landsat 5, 7, 8, 9	Max	Shawnee National Forest	TWI 0.190 slope 0.225 SPI_2024 0.166 max_summer_temp_2024 0.175 eastness 0.112 northness 0.131	PC1 0.218 PC2 0.181 PC3 0.151	No cropland layer in PCA
Landsat 5, 7, 8, 9	Min	Shawnee National Forest	TWI 0.198 slope 0.247 SPI_2024 0.122 max_summer_temp_2024 0.189 eastness 0.118 northness 0.126	PC1: 0.227 PC2: 0.179 PC3: 0.149	No cropland layer in PCA

*NDVI change taken out from final weights

Table A7
Variable Reclassification & Weighting

Variable	Method	Value Range	Rank/ Reclass	Weight (%) Shawnee National Forest	Weight (%) Kaskaskia
Slope	Natural Breaks	0 - 3.430 3.430 - 10.977 10.977 - 22.296 22.296 - 39.447 39.447 - 87.470	5 1 2 3 4	25	36
TWI	Natural Breaks	-0.025 - 7.294 7.294 - 10.481 10.481 - 14.731 14.731 - 18.272 18.272 - 30.077	4 1 2 3 5	20	34
Eastness	Natural Breaks	-1 - -0.686 -0.686 - -0.224 -0.224 - 0.208 0.208 - 0.663 0.663 - 1	5 4 3 2 1	12	5
Northness	Natural Breaks	-1 - -0.686 -0.686 - -0.224 -0.224 - 0.239 0.239 - 0.702 0.702 - 1	5 4 3 2 1	12	1
SPI	Manual Breaks	-1.630 - -0.723 -0.723 - -0.5 -0.5 - 0.5 0.5 - 0.7 0.7 - 2.042	5 3 1 3 5	12	17

Max. Temp.	Natural Breaks	33.550 - 35.432 35.432 - 36.342 36.342 - 37.127 37.127 - 37.942 37.942 - 41.550	1 2 3 4 5	19	1
Crop Proximity	Natural Breaks	0 - 128.223 128.223 - 470.149 470.149 - 983.039 983.039 - 1695.386 1695.386 - 3632.970	5 4 3 2 1	N/A	6

Value ranges are rounded to the nearest thousandth place (3rd decimal). Weights are derived from the PCA results for the Landsat minimum compositing dataset and are rounded to the nearest whole number due to the Weighted Overlay requiring integers.

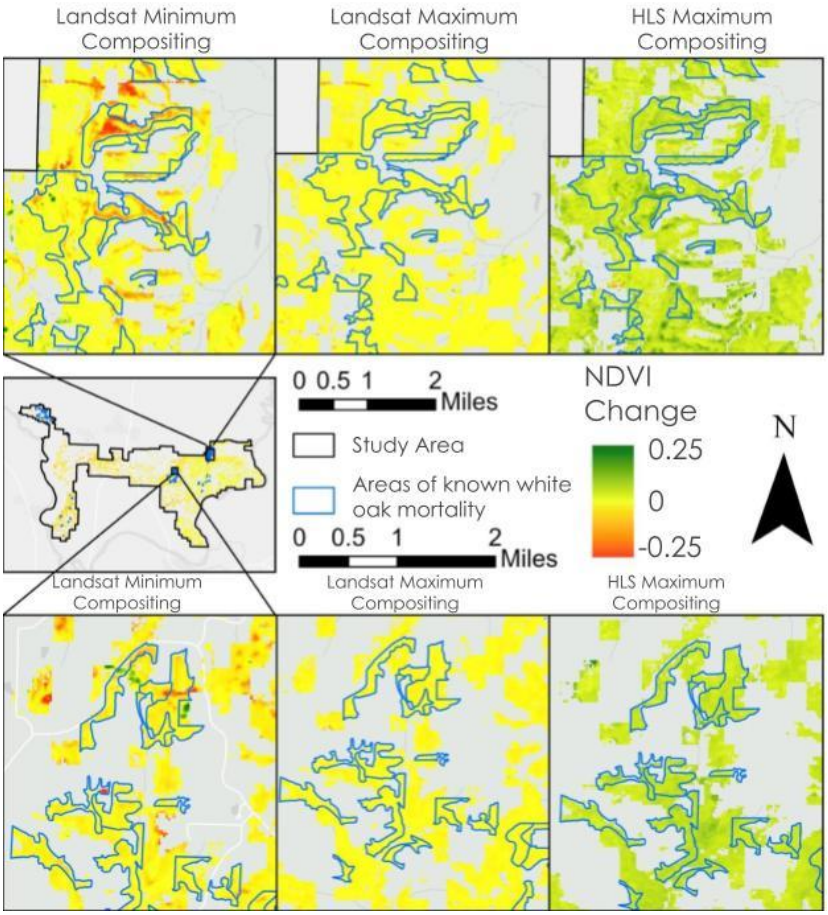

[Basemap CreditsMissouri DNR, Esri, TomTom, Garmin, FAO, NOAA, USGS, EPA, USFWS]

Figure B1. 2023 – 2024 NDVI change maps covering areas of known white oak decline in the Shawnee National Forest for Landsat minimum compositing (left), Landsat maximum compositing (middle), and HLS maximum compositing (right). HLS and Landsat data change maps were created with a scale of –0.25 to 0.25 with positive values indicating an increase in vegetation health and negative values suggesting a decrease. A negative NDVI change greater than 0.2 (orange/red) is considered significant and could be attributed to a forest disturbance, such as white oak mortality.

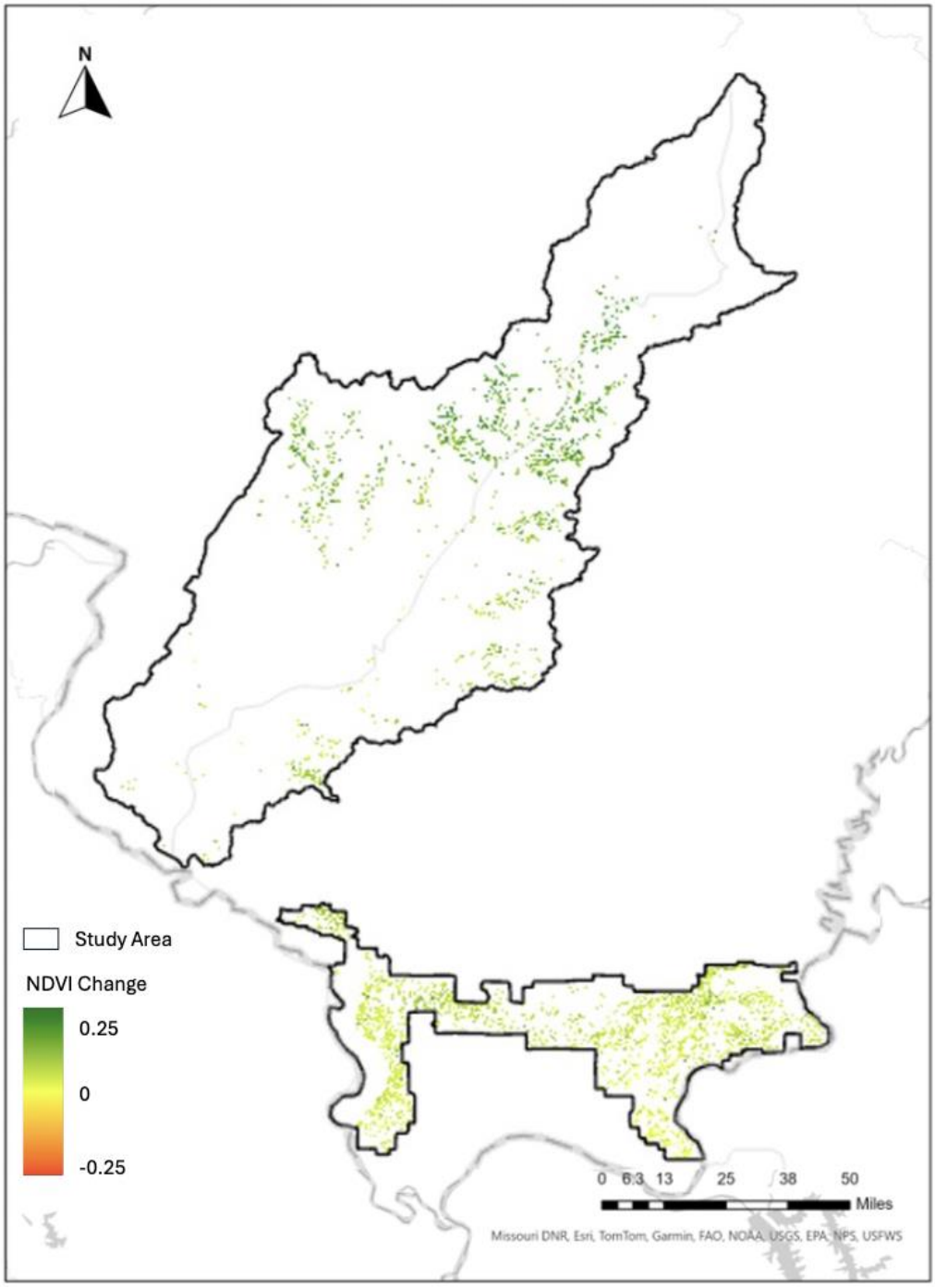

Figure B2. HLS 2023–2024 NDVI change map covering areas of known white oak decline in the Shawnee National Forest for HLS maximum compositing.

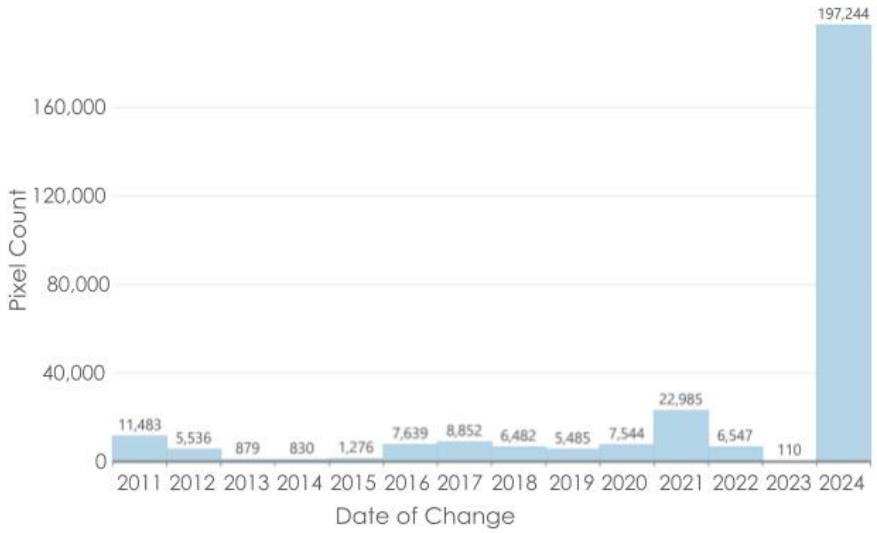

Figure B3. Histogram of LandTrendr Landsat minimum compositing results for 2010 – 2024 of the entire study area showing the number of changed pixels per year. A changed pixel for a given year occurred between the compositing dates of the growing season 07/15 – 09/30.

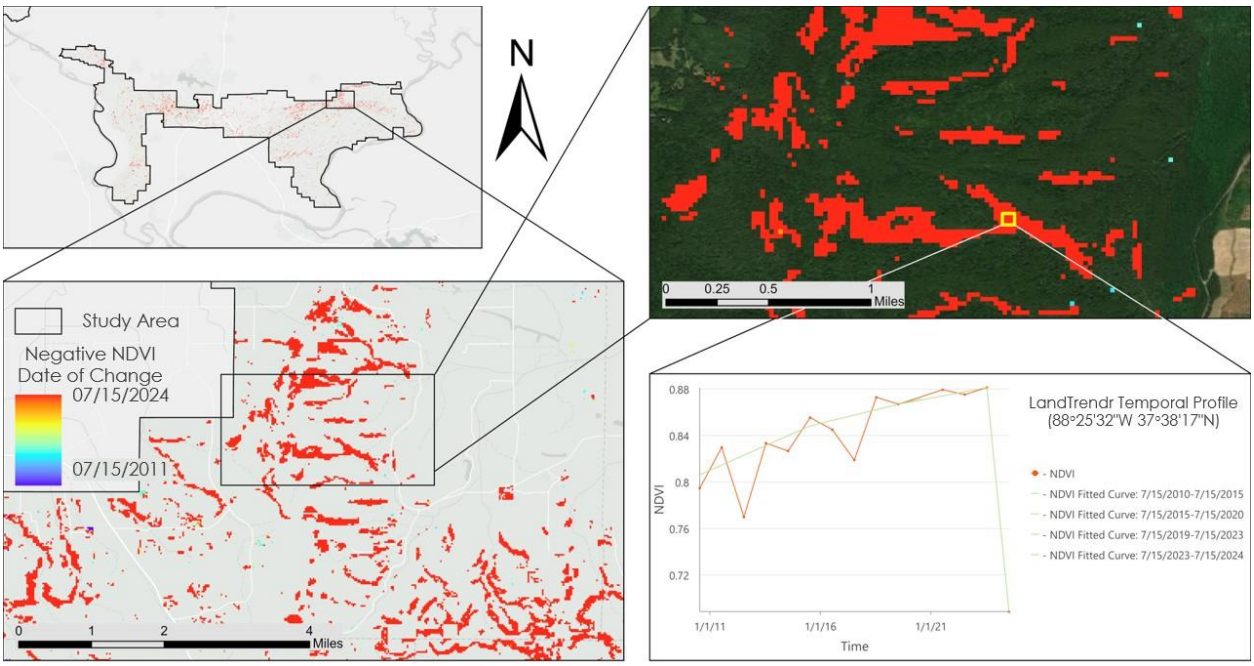

Esri, TomTom, Garmin, FAO, NOAA, USGS, EPA, NPS, USFWS, Esri, TomTom, Garmin, SafeGraph, GeoTechnologies, Inc, METI/NASA, USGS, EPA, NPS, USDA, USFWS, Maxar

Figure B4. LandTrendr Landsat minimum compositing date of change map from 2010 to 2024 for the Shawnee National Forest. Results are filtered for only negative NDVI change with a minimum magnitude of 0.1. A temporal profile of NDVI observation (red) with LandTrendr linear models (green) is included for an individual pixel (yellow square) that underwent change in the summer of 2024.

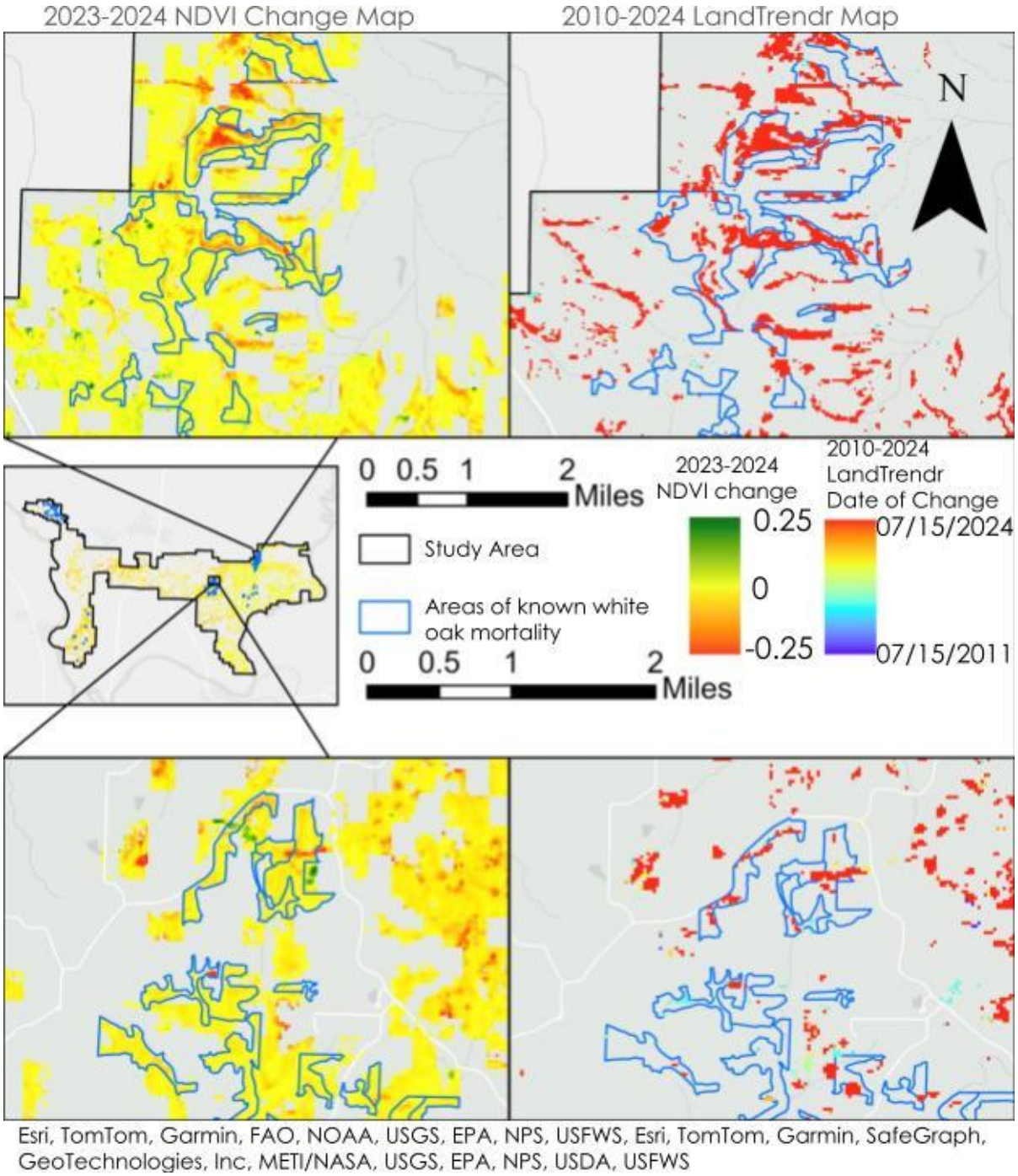

*Figure B5***.** 2023 – 2024 NDVI change maps (left) and LandTrendr date of change map from 2010 to 2024 (right) covering areas of known white oak decline in the Shawnee National Forest for Landsat minimum compositing results. LandTrendr results are filtered for decreasing NDVI with a change magnitude greater than 0.1 (Table A4).

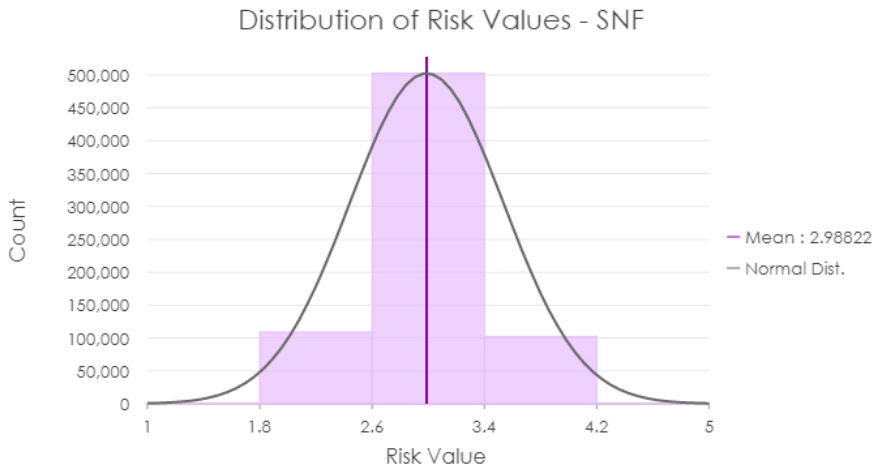

Figure B6. Decline risk value distribution, Shawnee National Forest. This figure shows the distribution of pixel counts for each risk level relative to the Shawnee National Forest, with each pixel corresponding to approximately 0.22 acres.

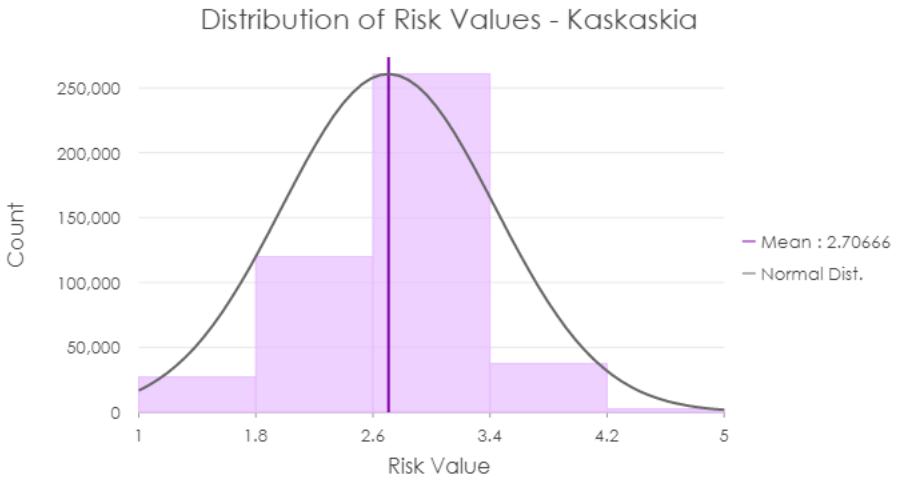

Figure B7. Decline Risk Value Distribution, Kaskaskia River Basin. This figure shows the distribution of pixel counts for each risk level relative to the Kaskaskia River Basin, with each pixel corresponding to approximately 0.22 acres.

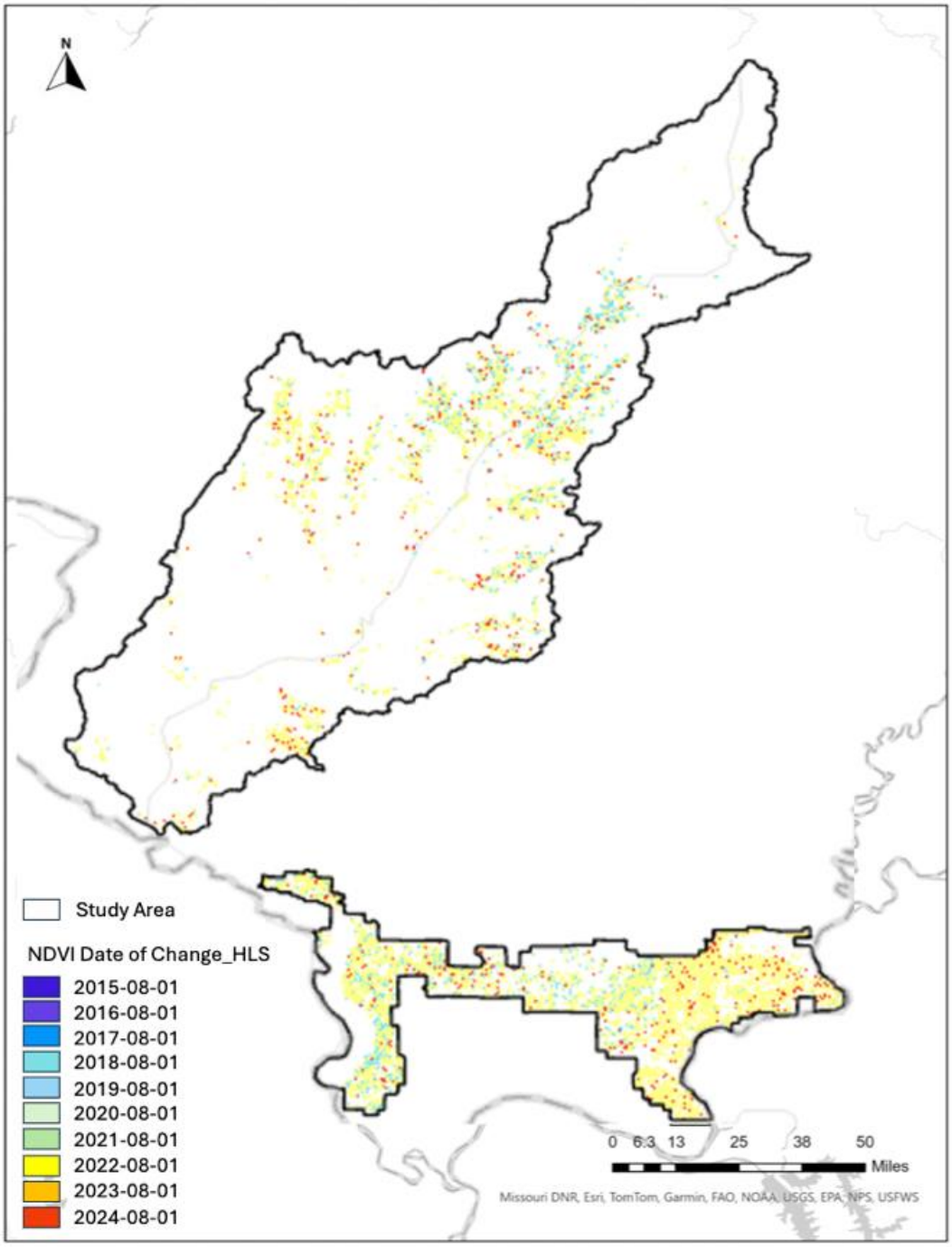

Figure B8. LandTrendr date of change map from 2015 to 2024 covering areas of known white oak decline in the Shawnee National Forest and Kaskaskia for maximum HLS compositing.

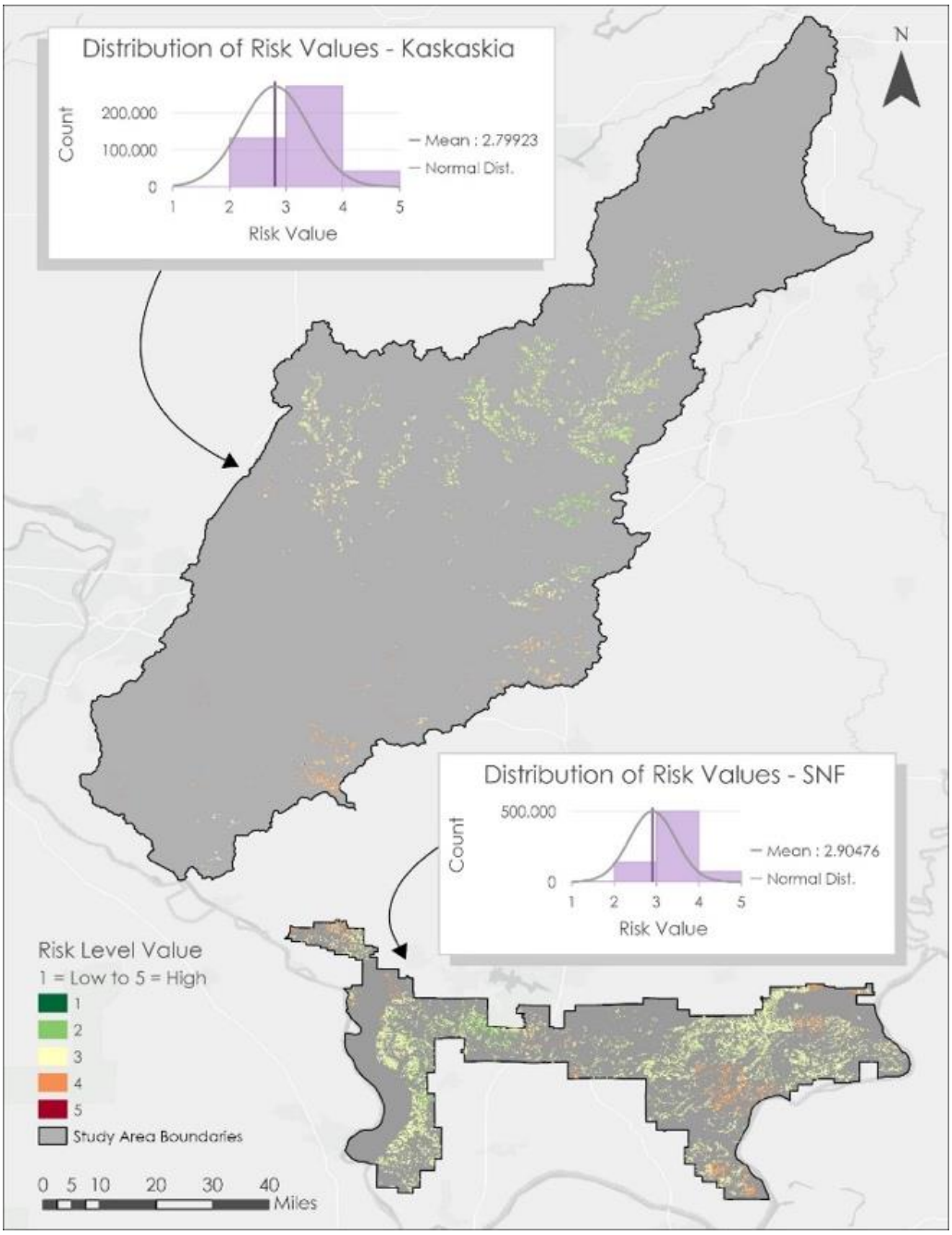

[Basemap CreditsMissouri DNR, Esri, TomTom, Garmin, FAO, NOAA, USGS, EPA, USFWS]

Figure B9. Oak decline risk map of the Kaskaskia River Basin and Shawnee National Forest using PCA values calculated based on HLS maximum NDVI compositing data. Green shades correlate to areas of low or low-moderate risk (1-2), the light-yellow shade matches areas of moderate risk (3), and the red shades correspond to areas of moderate-high to high risk (4-5). The inset maps highlight areas and patterns of decline.

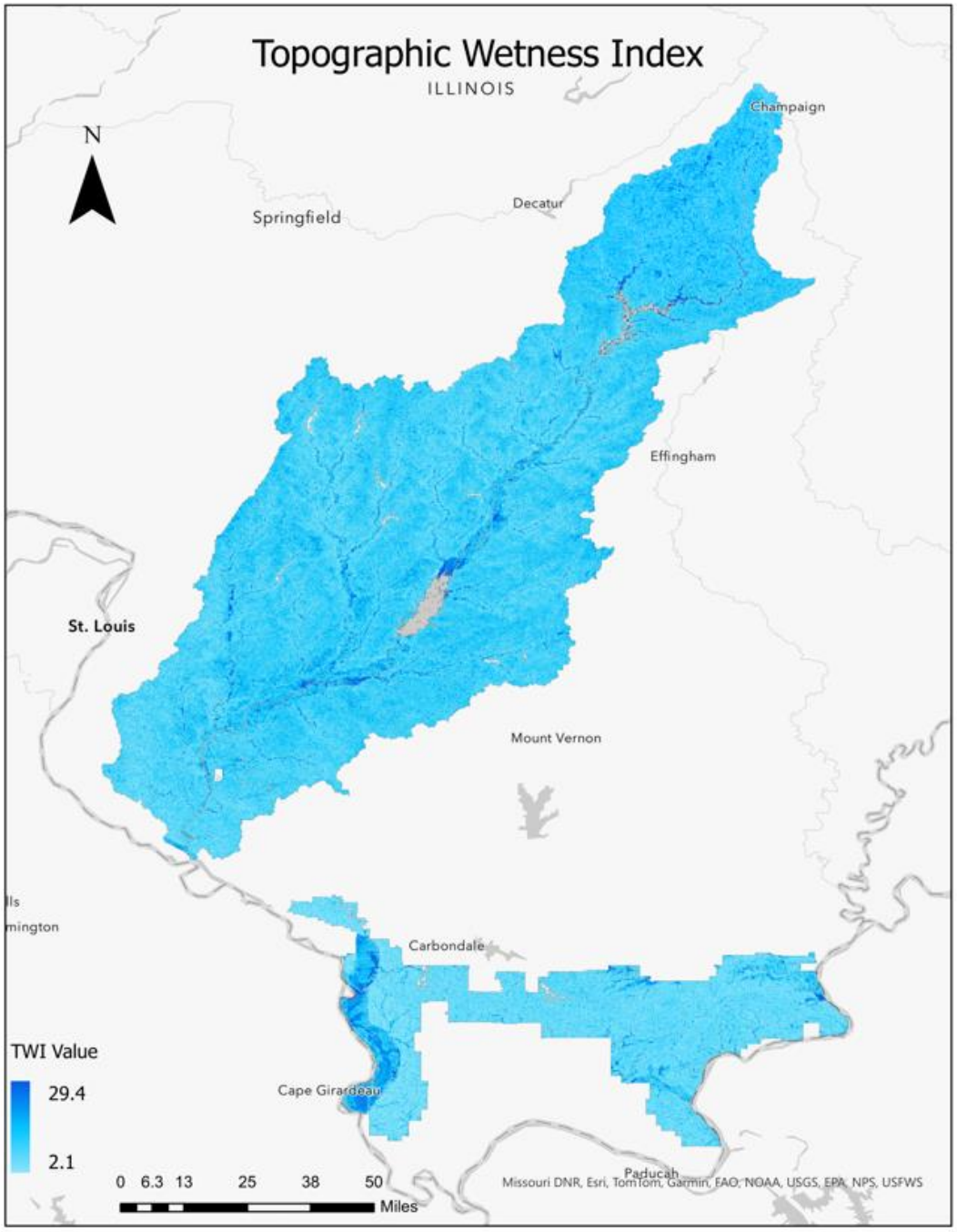

Figure B10. Topographic Wetness Index (TWI) values across the Kaskaskia River Basin (upper left) and Shawnee National Forest (lower right) in Illinois. Higher TWI values (darker blue) indicate areas more likely to accumulate water based on slope and upstream contributing areas. Scale bar shows TWI values ranging from 2.1 to 29.4.